Evaluation of Different Ni-Semiconductor Composites as Electrodes for Enhanced Hydrogen Evolution Reaction

Melisa J. Gomez[1,2], Victoria Benavente Llorente[1,2], Andrew Hainer[2], Gabriela I. Lacconi[1], Juan C. Scaiano[2], Esteban A. Franceschini[1,2]*, Anabel E. Lanterna[2]*

[1]INFIQC-CONICET, Departamento de Fisicoquímica – Facultad de Ciencias Químicas, Universidad Nacional de Córdoba, Ciudad Universitaria, 5000 Córdoba, Argentina
[2] Department of chemistry and Biomolecular Sciences, Centre for Advanced Materials Research (CAMaR), University of Ottawa, Ottawa, Canada

Table of Contents

55 Figure S1. EDS mapping of Ni|Nb_2O_5 catalyst.

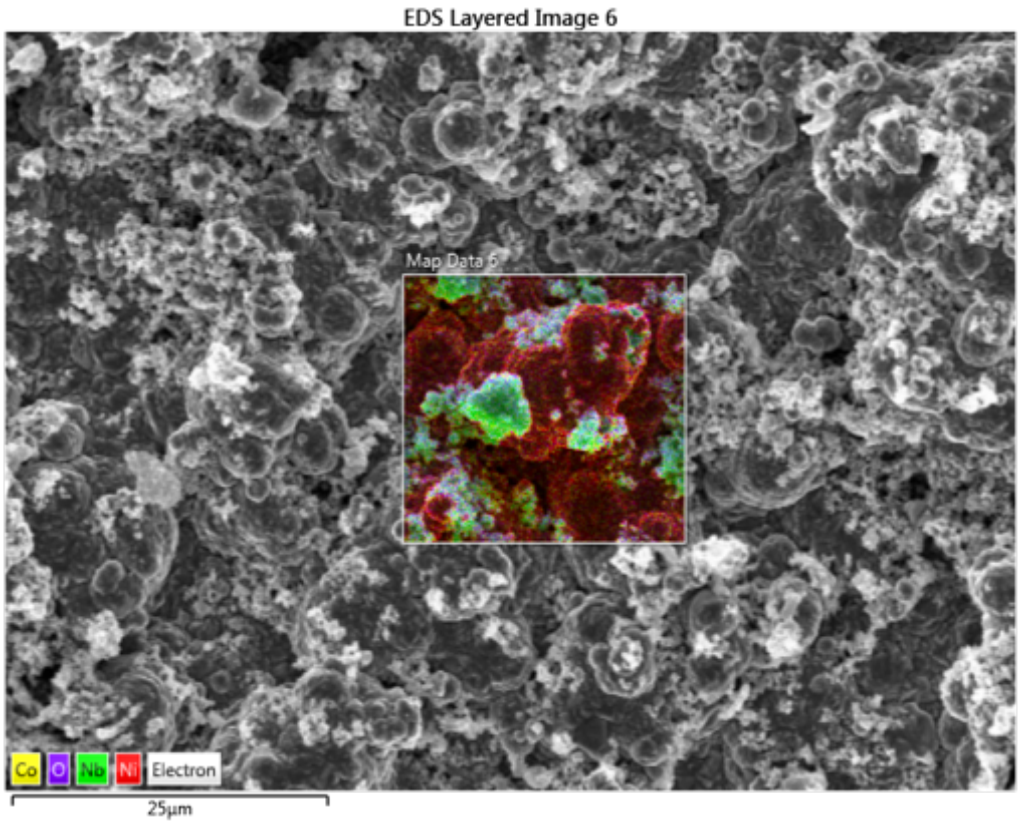

56

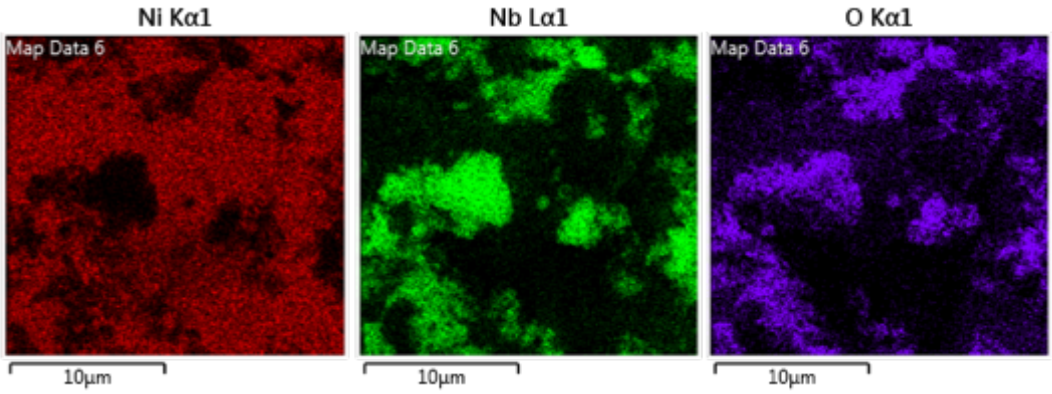

57

58 Figure S2. EDS mapping of Ni|$Nb_3(PO_4)_5$ catalyst.

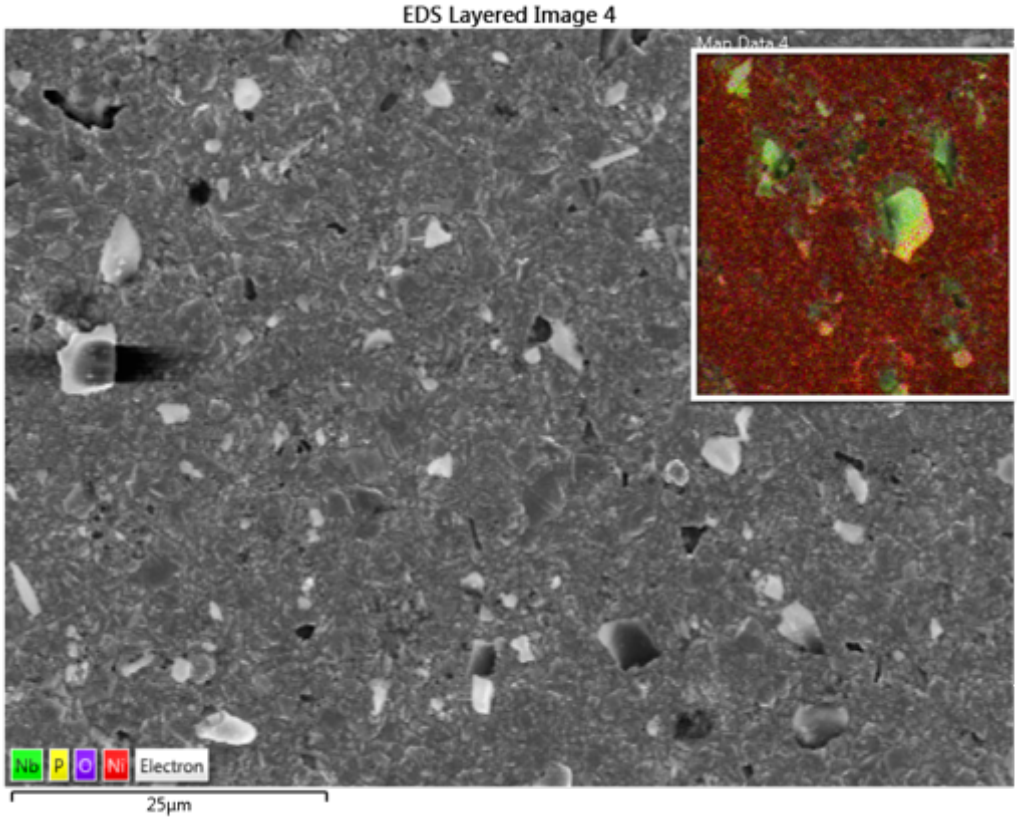

59

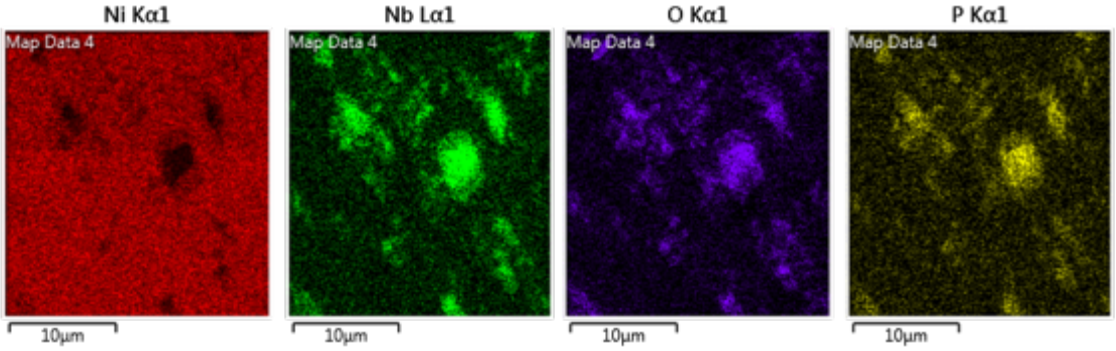

60

Figure S3. EDS mapping of Ni|Bi_2O_3 catalyst.

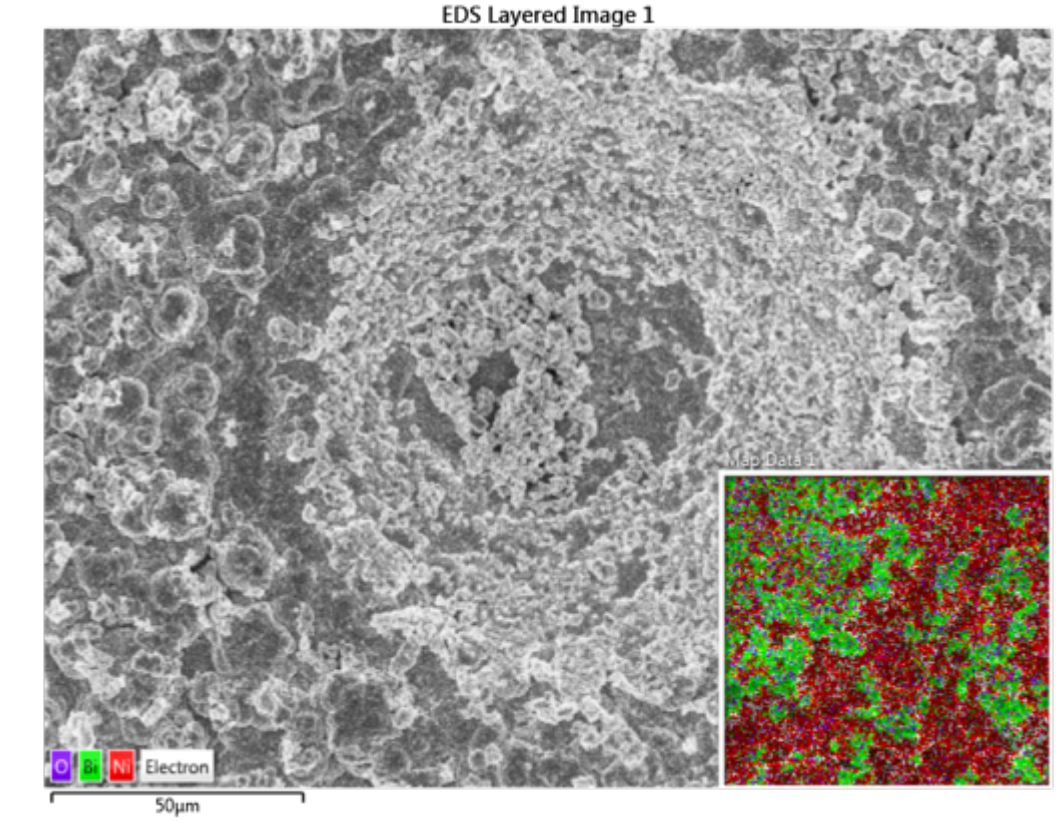

Figure S4. EDS mapping of Ni|WO_3 catalyst.

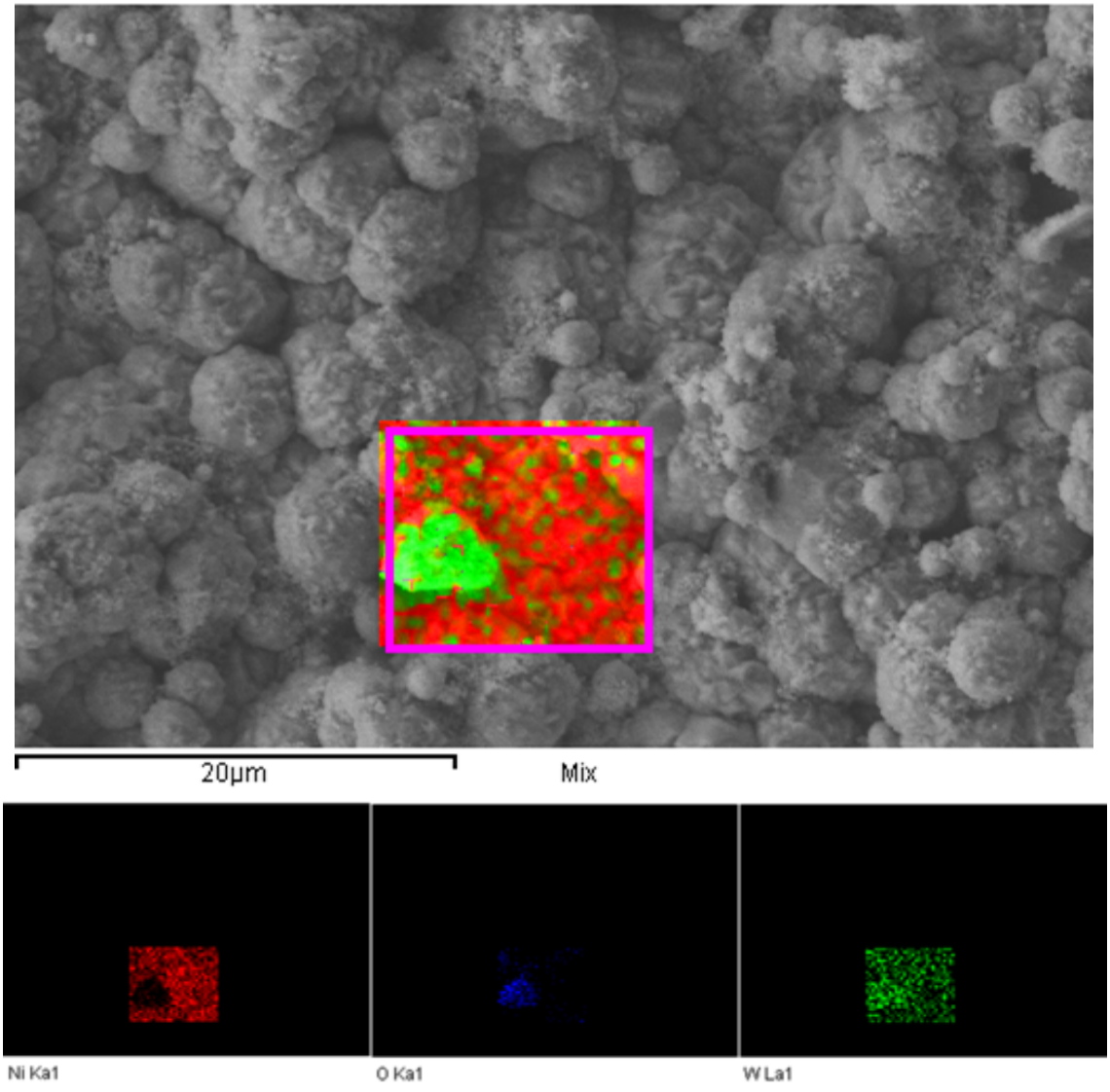

Figure S5. Confocal imaging of Ni|SC electrodes after ageing process (4h at -1.5 V vs SCE).

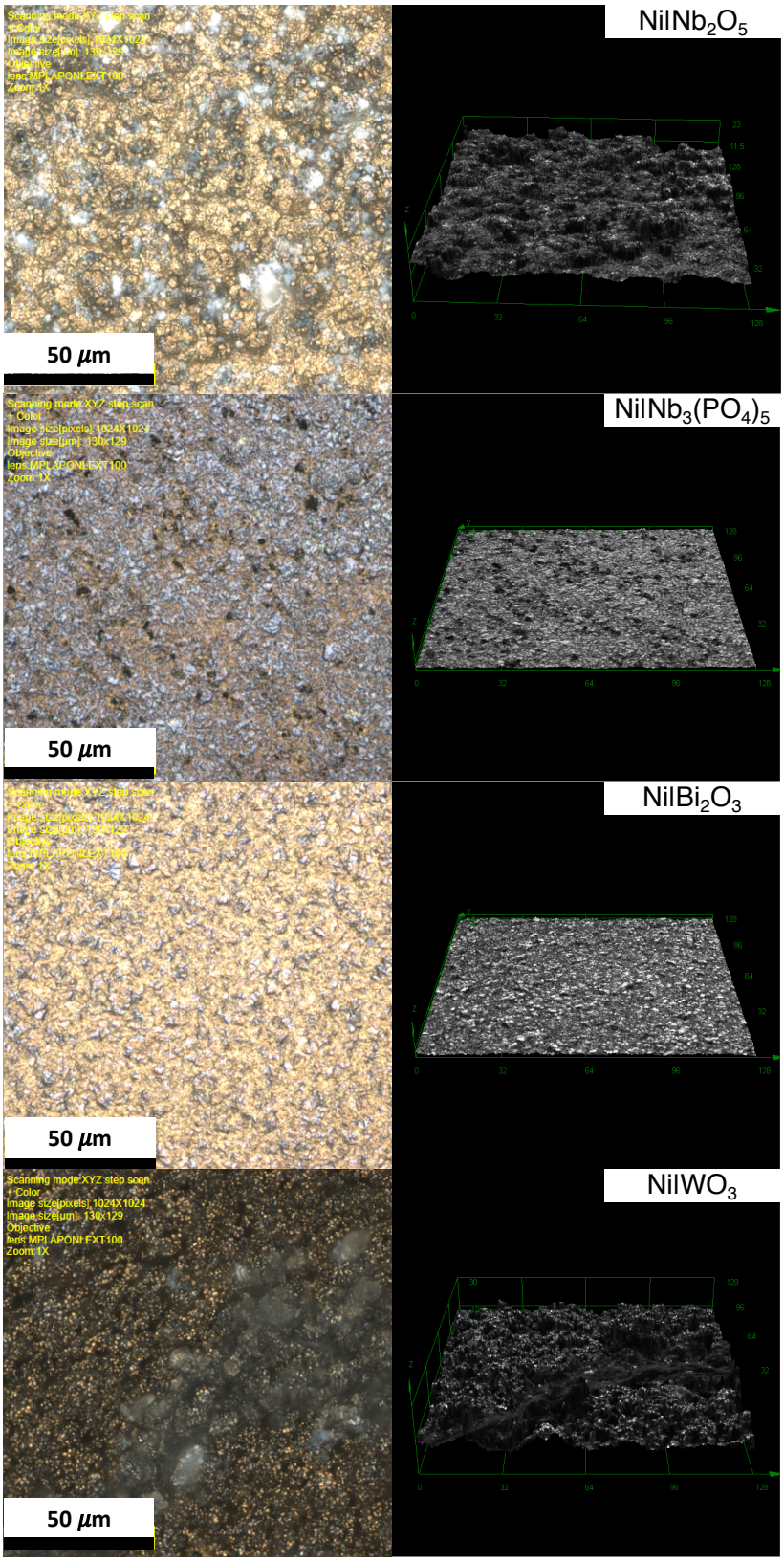

71 Table S1. Ni|SC electrodes total area calculated from confocal images in Figure S5 and
72 corresponding roughness factor.

	Total Area[a] / μm^2	R_f
Ni|Nb_2O_5	30,841	1.84
Ni|$Nb_3(PO_4)_5$	20,736	1.24
Ni|Bi_2O_3	23,213	1.38
Ni|WO_3	29,732	1.77

73 [a] Geometric area 16,784 μm^2.

Figure S6. XRD pattern from the semiconductors used. Note Nb_2O_5 orthorhombic [00-027-1313] and monoclinic crystalline structure [00-016-0053] as well as the amorphous nature of $Nb_3(PO_4)_5$ are described in literature[1].

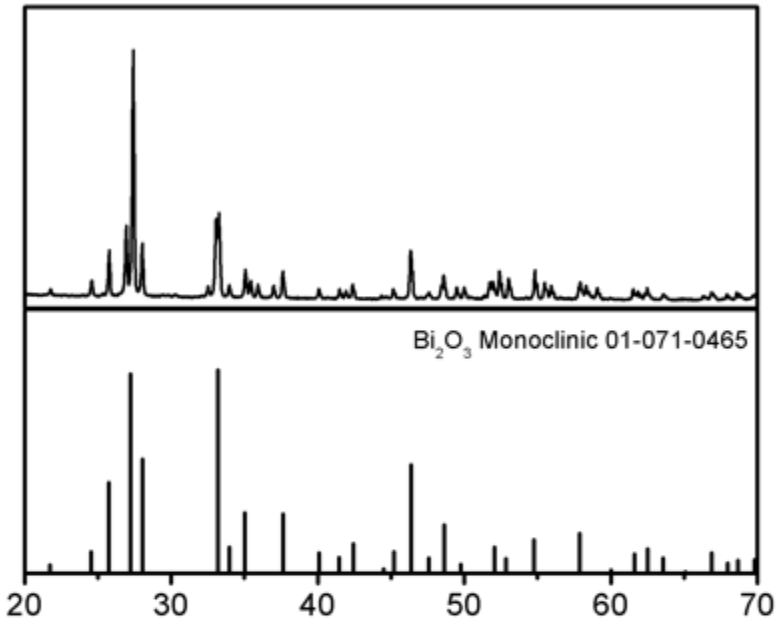

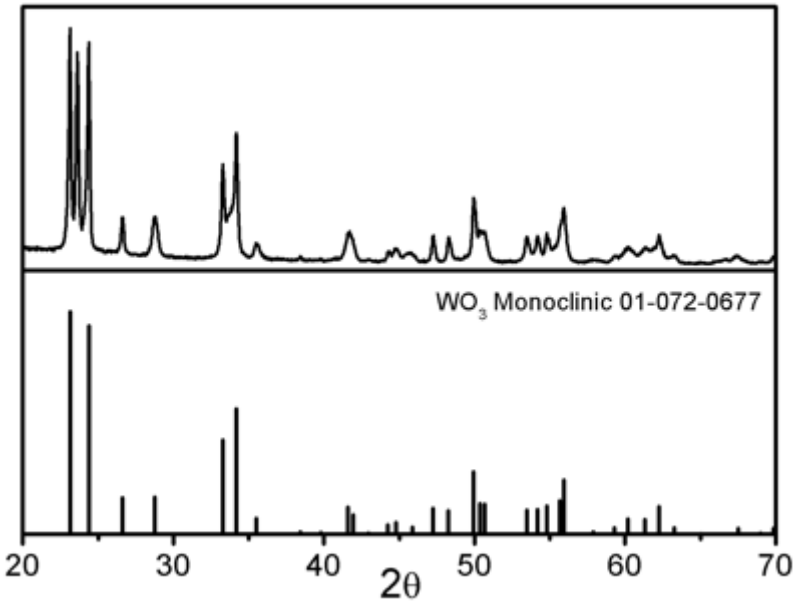

82 Table S2. Lattice parameters calculated from XRD analysis of the SC before (SC) and
83 after electrodeposition (Ni|SC).

	Plane	*2θ*		d spacing (Å)	
		SC	NiSC	SC	NiSC
WO_3	001	23.12	23.16	3.84	3.84
Nb_2O_5	040	22.65	22.61	3.92	3.93
Bi_2O_3	120	27.42	27.38	3.25	3.26
$Nb_3(PO_4)_5$	---	---	---	---	----

84

Figure S7. Ni 2p XPS spectra for Ni|SC electrodes.

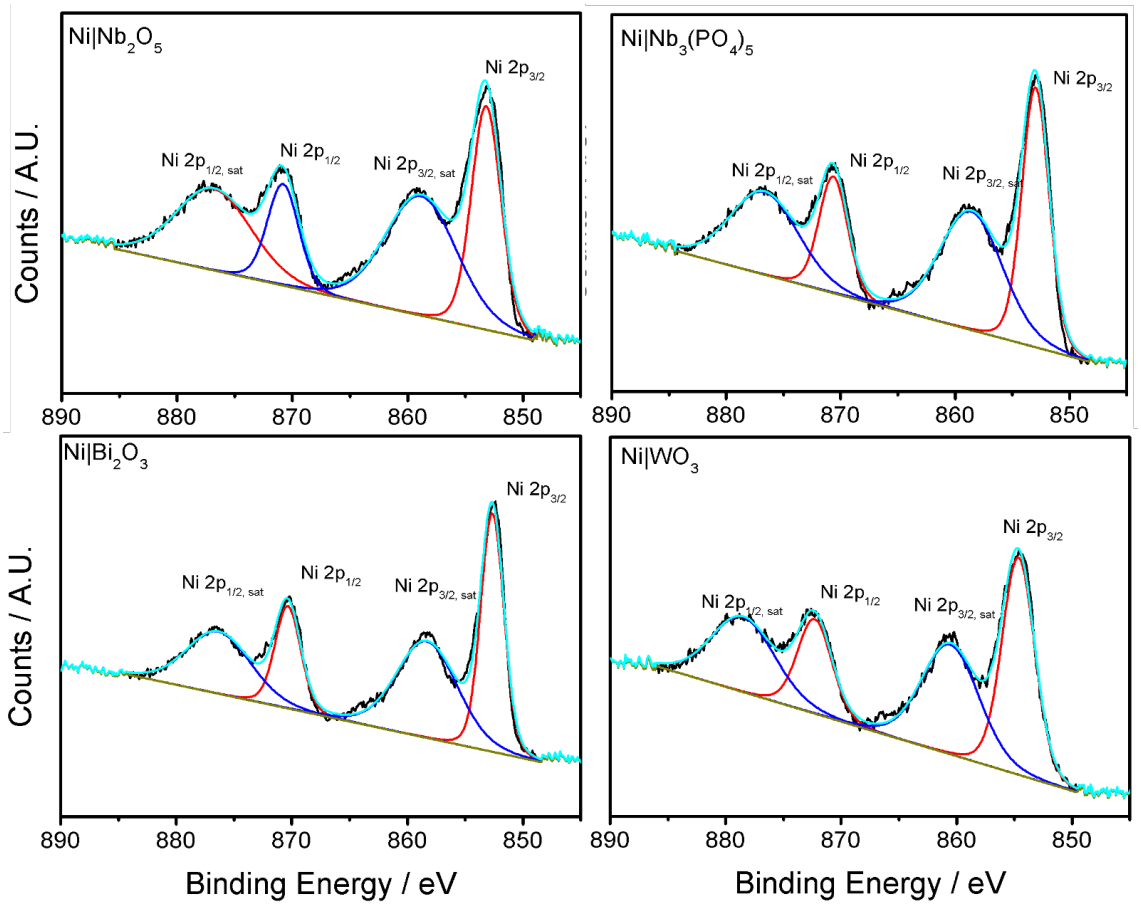

87 Figure S8. Ni LMM Auger spectra for Ni|SC electrodes.

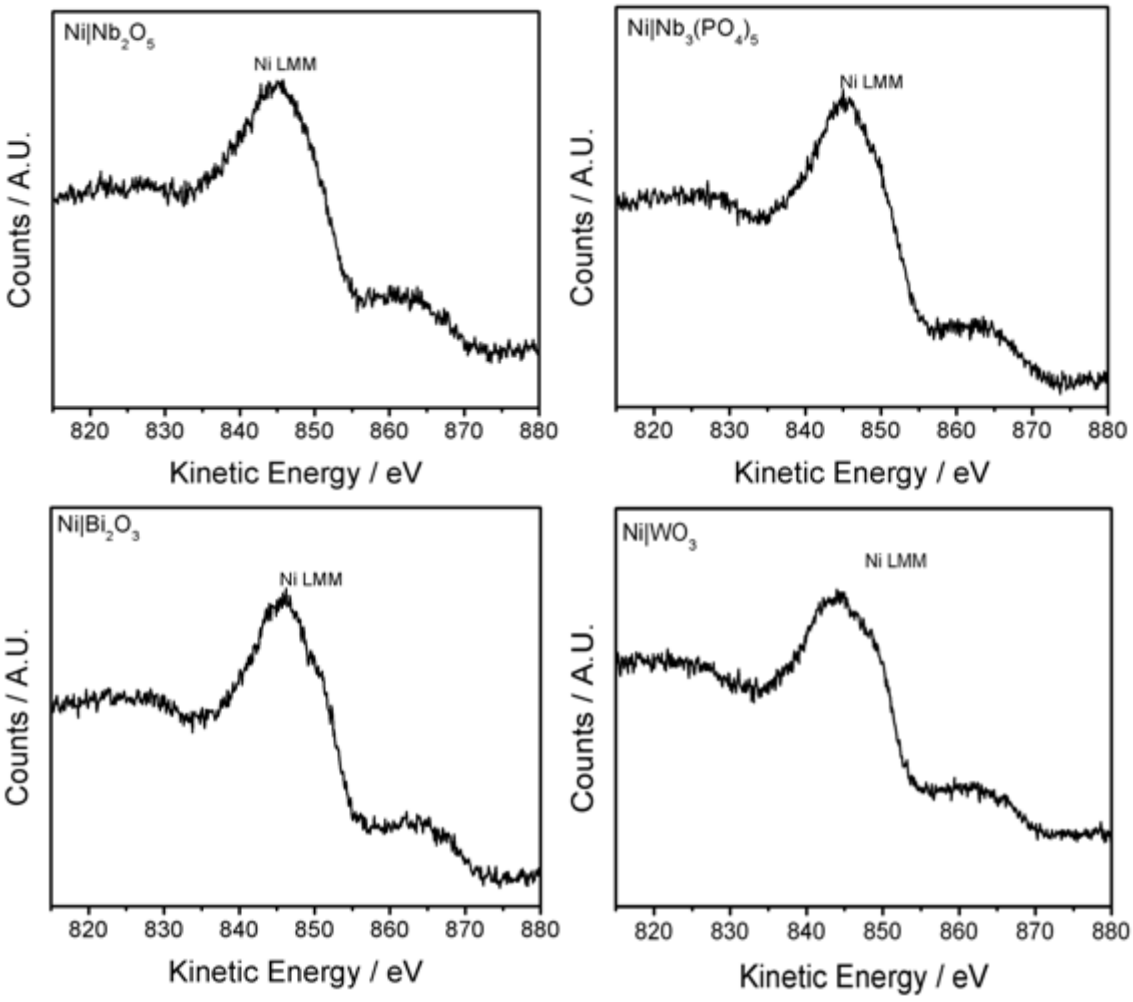

88

89

Figure S9. HR XPS spectra for Ni|SC electrodes.

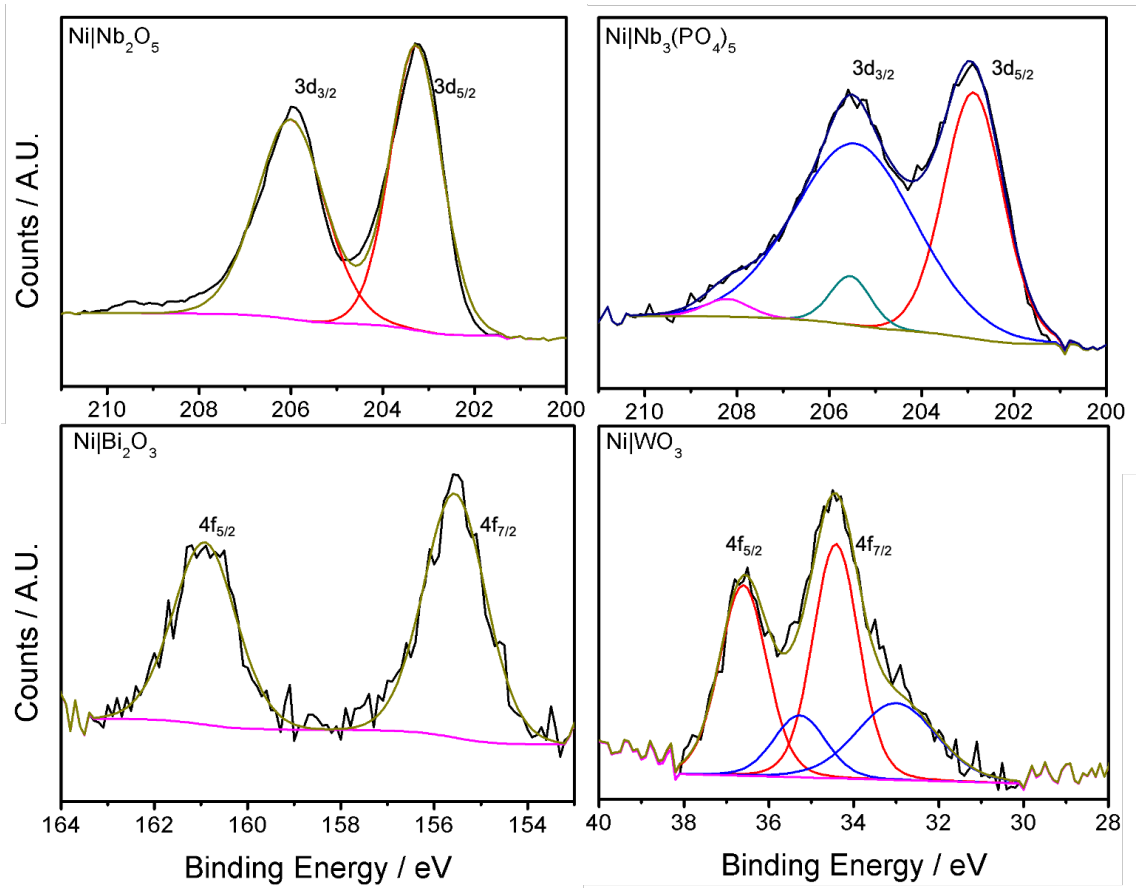

93 Table S3. XPS analysis for different Ni|SC.

Compound	Ni $2p_{3/2}$ peak		Ni $2p_{1/2}$ peak		Δ (eV)	Ni LMM Auger peak KE (eV)
	BE (eV)	ΔE_B (eV)	BE (eV)	ΔE_B (eV)		
Ni	852.73[2]	--	870.10[2]	--	17.37	846.22[3]
Ni|Nb_2O_5	853.20	0.47	870.81	0.71	17.61	845.79
Ni|$Nb_3(PO_4)_5$	852.98	0.25	870.64	0.54	17.67	844.99
Ni|Bi_2O_3	852.66	-0.07	870.35	0.25	17.69	846.19
Ni|WO_3	854.66	1.93	872.30	2.20	17.64	844.99

94
95

Figure S10. Oxidation/reduction peaks observed close to OP measured in 1.0 M KOH aqueous solution and recorded at 298 K at 10 mVs^{-1}.

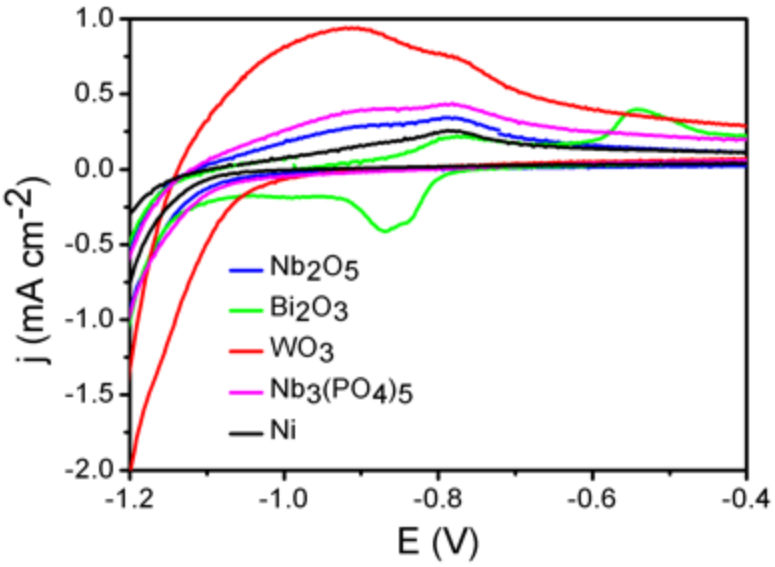

Figure S11. Tafel curves constructed from cyclic voltammograms measured in 1.0 M KOH aqueous solution and recorded at 298 K at 10 mVs^{-1}.

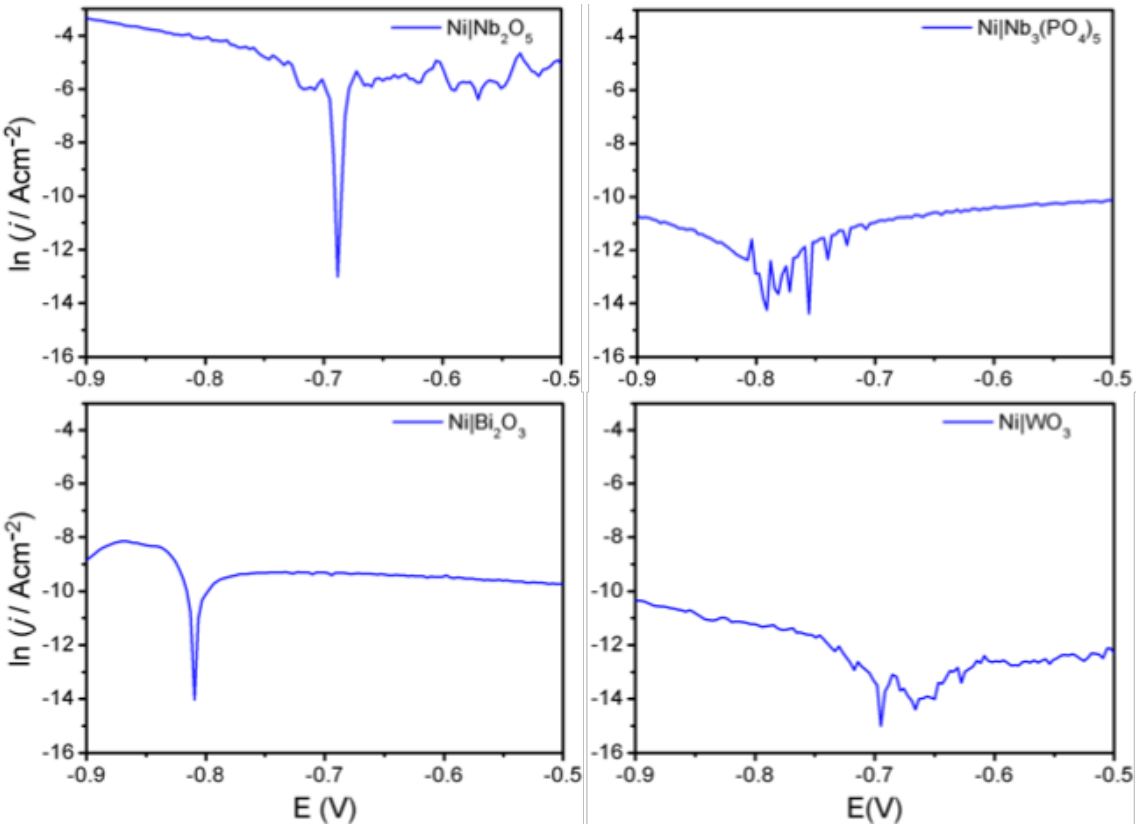

Figure S12. Cyclic voltammograms of freshly synthesised and aged Ni|SC catalysts measured in KOH 1.0 M and recorded at 298 K and 10 mVs^{-1}.

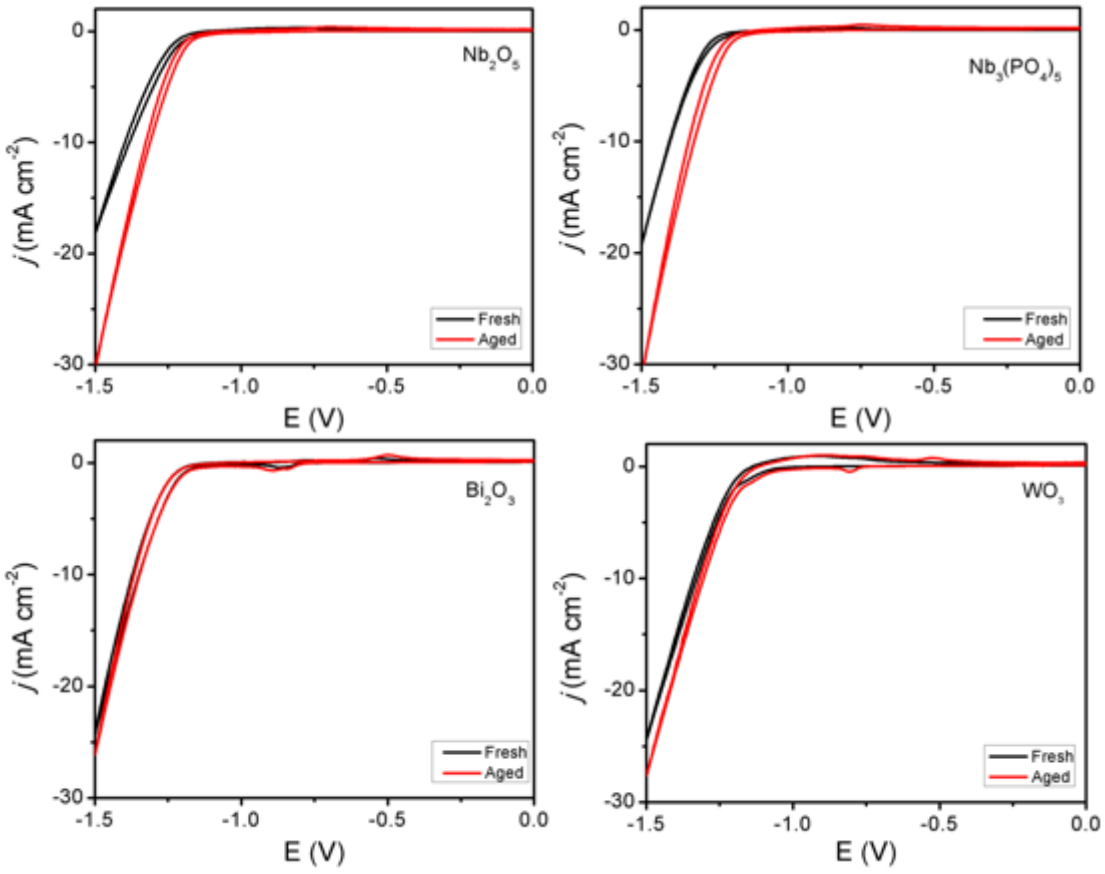

Figure S13. X-ray diffraction (XRD) pattern of Ni|SC electrodes after ageing process (4h at -1.5 V vs SCE).

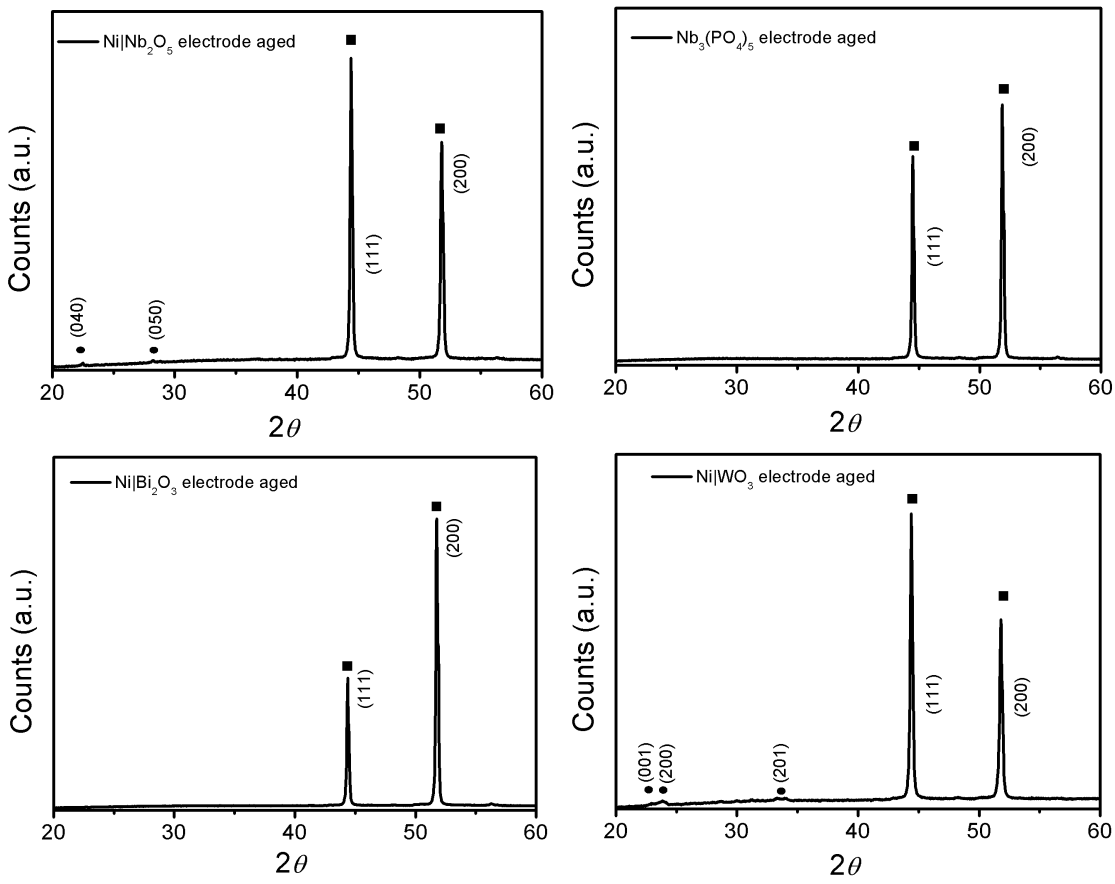

Table S4. Crystallite size calculated using the Scherrer equation for fresh and aged catalysts.

	Fresh / nm (± 1 nm)	Aged / nm (± 1 nm)	Plane
$Ni\|Bi_2O_3$	40.7	42.2	(111)
	40.0	41.0	(200)
$Ni\|Nb_2O_5$	42.7	44.0	(111)
	34.2	36.1	(200)
$Ni\|Nb_3(PO_4)_5$	44.8	43.9	(111)
	41.9	39.1	(200)
$Ni\|WO_3$	40.7	38.7	(111)
	32.9	34.9	(200)

Figure S14. Raman spectra of Ni|SC electrodes after ageing process showing no signals detected in the region where unreactive nickel hydroxide species are expected.[4]

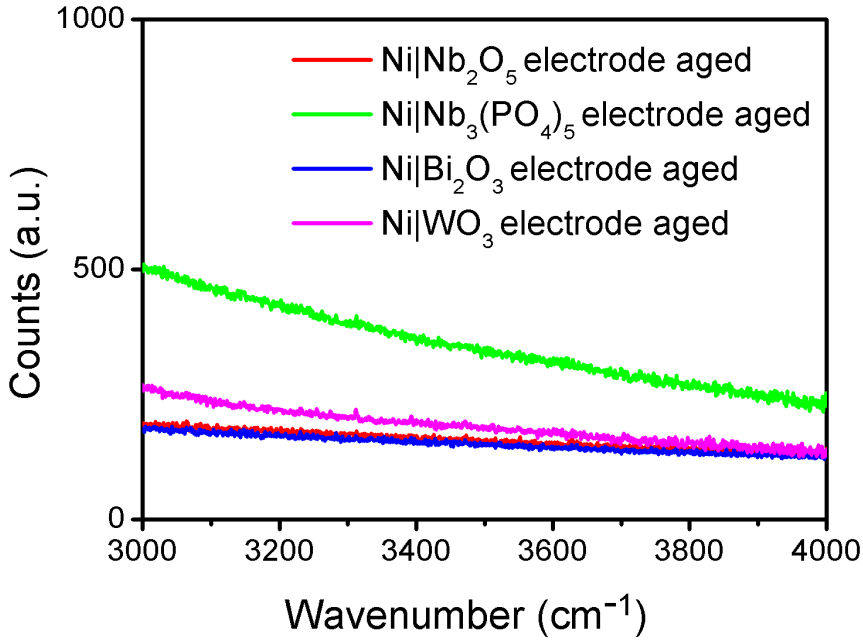

Figure S15. EIS measured for Ni|Bi_2O_3 electrodes at 298 K and −1.2 V (vs SCE) fitted with the equivalent circuit models: (a) Randles-CPE, (b) AHEC1CPE, (c) AHEC2CPE.

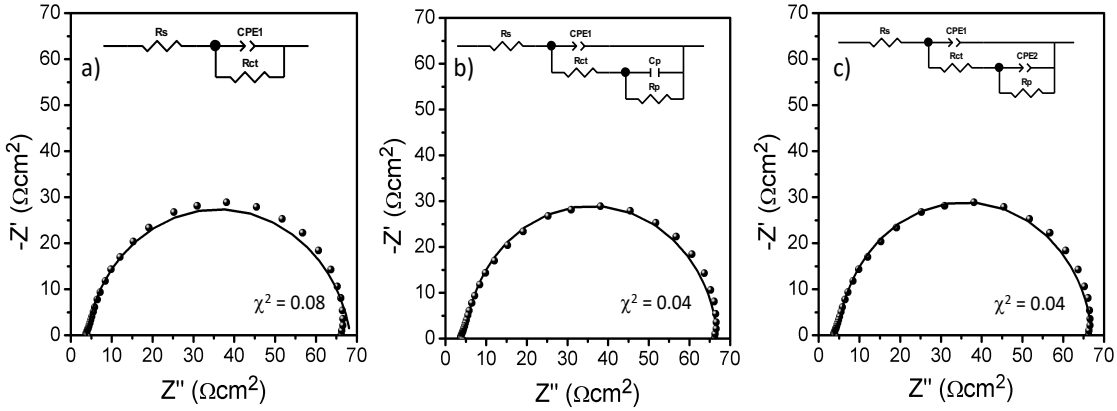

From the analysis of figures like Figure S14 prepared for each catalyst (Figure S15) we selected the AHEC1CPE model. The main limitation of Randles-CPE equivalent circuit is that it can only be used to fit one half-circle of the Nyquist plot which is commonly associated to the surface roughness[5-6], while the AHEC2CPE presents an excellent fit for two processes (increase of surface roughness and HER), although the use of a second CPE in replacement of the C_p lacks of physical significance, making the model inappropriate.

Figure S16. EIS measured for all Ni|SC electrodes at 25 °C and at different potentials fitted with the equivalent circuit models Randles-CPE, AHEC1CPE, and AHEC2CPE.

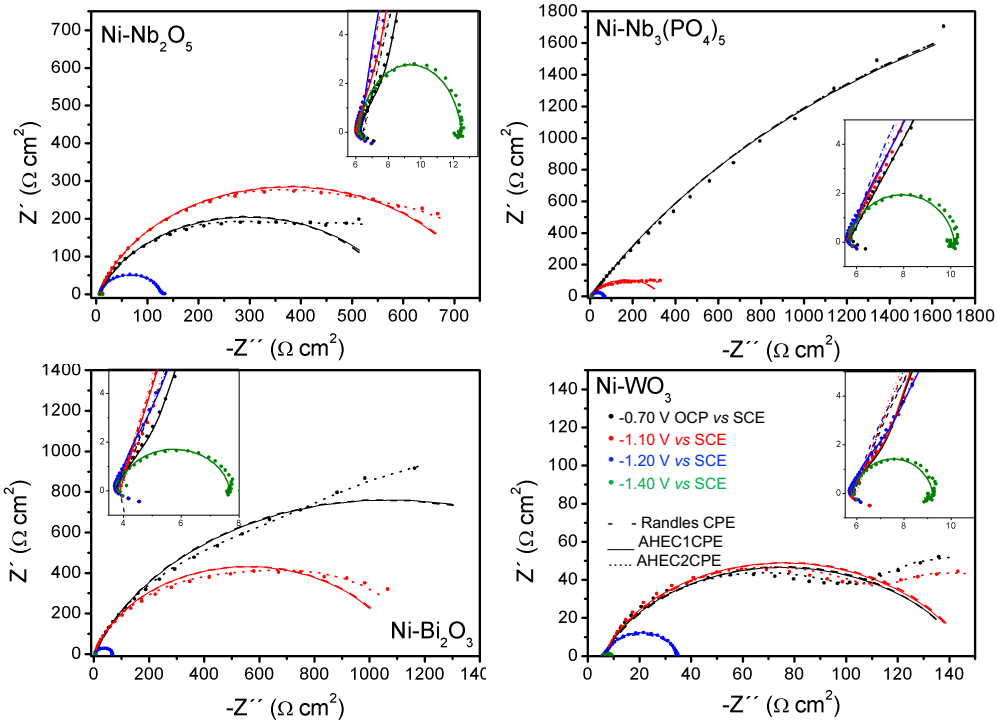

130 Figure S17. SEM imaging of Ni|Watts and Ni|SC electrodes after ageing process (4h at -
131 1.5 V vs SCE). Scale bar: 1 µm.

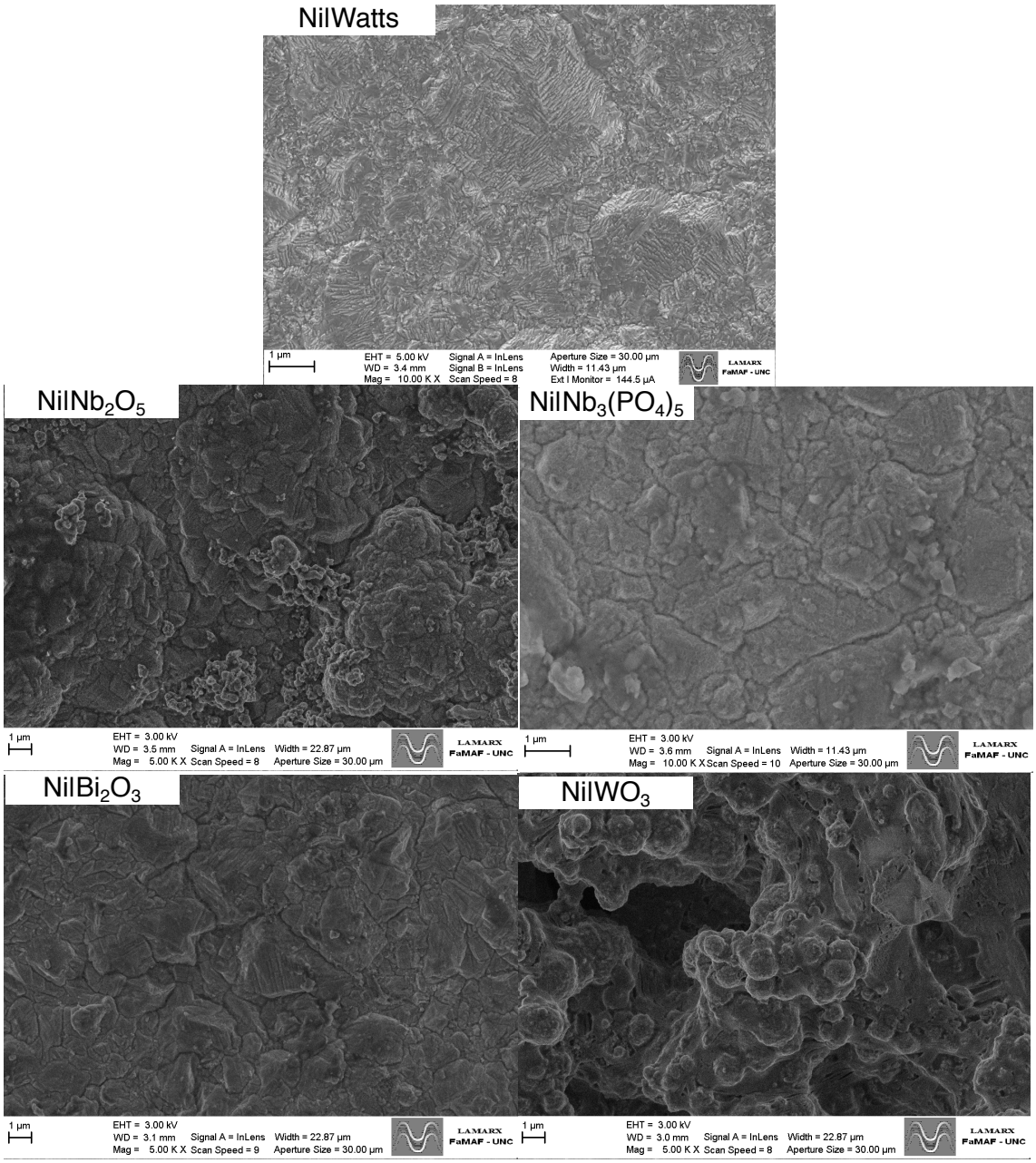

132

133 Figure S18. Comparison of SEM micrographs of Ni|$Nb_3(PO_4)_5$ before (left) and after
134 (right) ageing.

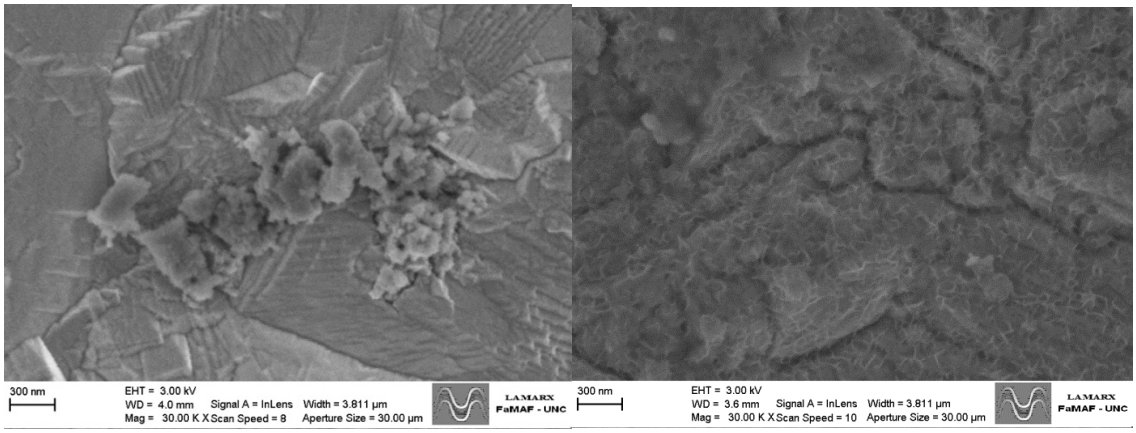

135

136

REFERENCES

[1] E. Franceschini, A. Hainer, A. E. Lanterna, *Int. J. Hydrogen Energy* **2019**, *44*, 31940-31948.

[2] A. N. Mansour, *Surf. Sci. Spectra* **1994**, *3*, 221-230.

[3] M. C. Biesinger, L. W. M. Lau, A. R. Gerson, R. S. C. Smart, *Phys. Chem. Chem. Phys.* **2012**, *14*, 2434-2442.

[4] D. S. Hall, D. J. Lockwood, S. Poirier, C. Bock, B. R. MacDougall, *J. Phys. Chem. A* **2012**, *116*, 6771-6784.

[5] A. Lasia, A. Rami, *J. Electroanal. Chem.* **1990**, *294*, 123-141.

[6] L. L. Chen, A. Lasia, *J. Electrochem. Soc.* **1991**, *138*, 3321-3328.